

Preparation and characterization of organic-inorganic hybrid nanomaterials using polyurethane-*b*-poly[3-(trimethoxysilyl) propyl methacrylate] via RAFT polymerization

S. Z. Guo, C. Zhang, W. Z. Wang, T. X. Liu*

Key Laboratory of Molecular Engineering of Polymers of Ministry of Education, Department of Macromolecular Science, Laboratory of Advanced Materials, Fudan University, Shanghai 200433, P. R. China

Received 13 May 2009; accepted in revised form 11 October 2009

Abstract. A series of novel block-type amphiphilic copolymers have been prepared by copolymerizing methacrylate end-capped oligo-urethane and 3-(trimethoxysilyl) propyl methacrylate (TPM) via the sol-gel process. Copolymers with well-defined end groups and narrow polydispersity were prepared through Reversible Addition Fragmentation Chain Transfer (RAFT) polymerization. As-synthesized copolymer was characterized ^1H nuclear magnetic resonance (^1H NMR), gel permeation chromatography (GPC), Fourier transform infrared (FTIR). The copolymer precursors self-assembled in form of spherical micelles (in selective solvents) have been hydrolyzed and then condensed via sol-gel process in order to generate polyurethane-silica (PU-SiO₂) hybrid materials. The hybrid copolymers thus prepared possess excellent thermal stability and mechanical property. The structures and properties of the copolymer precursors and their hybrid copolymers were characterized by thermogravimetric analysis (TGA), tensile test and atomic force microscopy (AFM).

Keywords: nanomaterials, polyurethane, organic-inorganic hybrids, RAFT polymerization, self-assembly

1. Introduction

Self-assembly of amphiphilic diblock copolymers and associated nano-science afford unique opportunities to create revolutionary material combinations. Wide variety of aggregates (e.g., spheres, vesicles, large compound spheres and vesicles) with different sizes can be obtained in selective solvents through sol-gel process [1–8]. These novel materials can have improved (mechanical, thermal etc.) properties arising from the synergism of the components and their interesting morphologies. In addition, well-defined polymer-nanoparticle hybrids with controlled architectures also have promising potential applications such as microreactors, microcapsules, and drug delivery systems [9–14].

Recently, increasing attention has been paid to the incorporation of an inorganic network by covalent bond such as a silica phase into an organic polymer matrix to produce monolithic, transparent hybrid nanoballs without macroscopic phase separation. Researchers have shown that these nanoballs may be incorporated as building-block fillers or cores into other polymers to form hybrid organic-inorganic copolymers with improved compatibility and hence elasticity. In addition, optimal dispersion of silica nanoballs within the polymer serves as reinforcing nanofiller with high surface coverage. Up to now, a large number of methods have been reported to prepare organic-inorganic hybrid nanoballs. One of the methods mentioned above, the

*Corresponding author, e-mail: txliu@fudan.edu.cn

© BME-PT

sol-gel method, permits access to hybrid nanoballs through a very simple one-pot procedure. TPM with reactive trimethoxysilane groups is widely used in the preparation of organic-inorganic hybrid nanomaterials [15–19]. With a base catalyst, the R-Si(OCH₃)₃ groups can be easily hydrolyzed into R-Si(OH)₃ which can subsequently transform into cross-linked polysilsesquioxane nanocages by condensation, thus producing organic-inorganic hybrid nanoballs [7, 20, 21]. Recently, some research interests have sparked in the studies of self-assembly of copolymers based on poly[3-(trimethoxysilyl) propyl methacrylate] (PTPM). For example, Chen et al. reported the preparation and self-assembly behavior of novel organic-inorganic hybrid nanoparticles with a complex hollow structure based on a reactive amphiphilic diblock copolymer, poly(ethylene oxide)-*b*-poly[3-(trimethoxysilyl) propyl methacrylate] (PEO-*b*-PTPM) [22].

Polyurethanes (PU), as organic matrices, have received most attention for their versatile properties and a variety of starting materials. Therefore, the tailor-made properties of this class of materials can be obtained from well-designed combinations of monomeric materials, catalysts, auxiliary compounds. Polyurethanes can be tailored to meet the highly diversified demands of modern technologies such as coatings, adhesives, reaction injection molding, fibers, foams, rubbers, and thermoplastic elastomers. The linear structures of segmented PU take the form of (A-B)_n. The soft segment part B represents the polyester or polyether macrogels with molecular weights ranging from 1000 to 3000; and the hard segment part A is consisted of low-molecular weight diol or diamine being able to react with diisocyanate. Because of the incompatibility between the hard segments and the soft ones, PU undergoes microphase separation resulting in a hard-segment domain, soft-segment matrix, and urethane-bonded interphase. The hard-segment domains act as physical cross-links in the soft-segment matrix. The primary driving force of phase separation is the strong intermolecular interaction of the urethane units, which are capable of forming intermolecular hydrogen bonds. Upon mechanical deformation, a portion of the soft segments is stressed by uncoiling and the hard segments align themselves in the stress direction. The reorientation of the hard segments and consequently the powerful hydrogen bonding contribute to enhance the

tensile strength, elongation and tear resistance values. Some polyurethane-silica hybrids have been prepared and reported, such as PU composites containing alkoxysilane groups [7, 23], PU composites containing POSS (polyhedral oligomeric silsesquioxane) nanocages [24, 25]. In the present paper, inorganic-organic diblock copolymers are prepared by incorporating 3-(trimethoxysilyl) propyl methacrylate (TPM) to vinyl-terminated PU macromonomers.

Recent progress in controlled ‘living’ free-radical polymerization techniques, such as atom transfer radical polymerization (ATRP) [26], nitroxide-mediated radical polymerization (NMP) [27], and reversible addition-fragmentation chain transfer (RAFT) polymerization [28–30], has created new avenues for the synthesis of structured polymers with predefined molecular weights, well-defined end groups, and narrow polydispersity. Polymerizations of vinyl monomers via RAFT have already been reported [31]. It may be of interest to prepare polyurethane-silica hybrid polymers using RAFT, since the copolymer of TPM and PU could combine the reactive groups, nontoxic, highly biocompatible and inorganic properties of TPM with the properties of PU.

Herein, the present study focuses on the synthesis of a diblock copolymer of PU-*b*-PTPM using cumyl dithiobenzoate (CDB) based RAFT in tetrahydrofuran (THF) solution and investigation of the self-assembly behaviors of the resultant polymer in THF/methanol mixture. As is known, PU-*b*-PTPM copolymer can form micelles with PU as the corona and the hydrophobic block as the core; and the siloxane part on the copolymer precursor can form a kind of stable polysilsesquioxane nanocages by hydrolysis and condensation reaction. This inorganic nanocages incorporated into the PU matrix by covalent bond increase the compatibility between the PU matrix and inorganic parts, thus improve the properties of the hybrid nanocomposites.

2. Experimental

2.1. Materials

Dibutyl tin dilaurate, 2-hydroxypropyl acrylate (HPA), methyl ethyl ketone (MEK), THF (purchased from Sinopharm Chemical Reagent Co., Ltd China), isophorone diisocyanate (IPDI, from Alfa

Aesar) and isophorone diamine (Fluka), 3-(trimethoxysilyl) propyl methacrylate (TPM, purchased from Acros Organics), 2,2'-Azobisisobutyronitrile (AIBN, purchased from Shanghai Shishihewei Chemical Co.) were used without further purification. Poly(diethylene adipate) (PDA, purchased from Jiangdu Longchuan Wear-Resistant Polymer Materials Co., Ltd China) was dried under vacuum at 80°C for 1 h before use. Cumyl dithiobenzoate (CDB) was synthesized according to the literature procedure [32] and recrystallized twice using petroleum ether. All the rest materials were purchased from Aldrich and used as received unless stated otherwise.

2.2. Synthesis of double-bond end-capped polyurethane macroinitiator

IPDI (29.96 mmol) and PDA (14.98 mmol) were added into a reaction flask with MEK as solvent, followed by heating up to 75°C, and then the solution (solid content: 90 wt%) was reacted in the presence of dibutyl tin dilaurate (0.02 wt%) at the same temperature for 3 h to synthesize the NCO-terminated prepolymer. After MEK was injected into the flask to adjust the solid content to be 30 wt%, the solution was allowed to cool down to room temperature. Then, the chain extender IPDA (12.91 mmol) was slowly charged into the system. After 1 h, HPA (2.00 mmol) was added into the system at 50°C and the temperature was kept there for 10 h, and polyurethane macroinitiator with vinyl end-capped was prepared. Then, the obtained solution was cooled down to room temperature and immediately used for further copolymerization with TPM.

2.3. Synthesis of copolymer of PU-*b*-PTPM by RAFT

The polymerization procedure and the recipes are presented in Figure 1 and Table 1, respectively. The polymerization procedure mediated by CDB

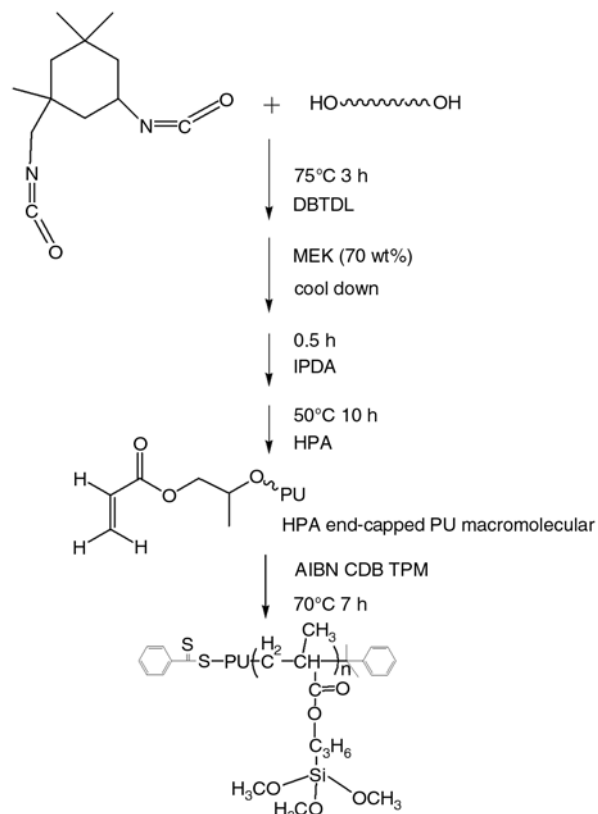


Figure 1. Synthesis procedure of PU-*b*-PTPM

procedure was as follows (as shown in Figure 1): polyurethane macroinitiator (5.0 g, $1.75 \cdot 10^{-4}$ mol), AIBN (25 mg, $1.52 \cdot 10^{-4}$ mol), TPM (0.5 g, $2.01 \cdot 10^{-3}$ mol) and CDB (76 mg, $2.79 \cdot 10^{-4}$ mol) were transferred into a 25 ml flask, and the THF solution was degassed with three cycles of freezing pump thawing to remove the oxygen. The reaction mixture was then warmed to 70°C. After 7 h, the polymerization was stopped by cooling to room temperature by liquid nitrogen and then the flask was opened. The mixture was soon precipitated into 250 ml of anhydrous methanol to remove the catalyst such as dibutyl tin dilaurate and unreacted TPM. Finally, the PU-*b*-PTPM diblock copolymers were obtained. The contents of TPM monomer in the copolymers can be roughly estimated to be 14, 19 and 32, respectively, by GPC results. The copolymers thus obtained were labeled as PU-A, PU-B, and PU-C correspondingly.

Table 1. Recipes for synthesis and the results obtained from GPC experiments

Code	PU [mol]	TPM [mol]	CDB [mol]	AIBN [mol]	M _w [Dalton]	PDI
PU	$1.75 \cdot 10^{-4}$	–	$2.79 \cdot 10^{-4}$	$1.52 \cdot 10^{-4}$	28600	1.63
PU-A	$1.75 \cdot 10^{-4}$	$2.01 \cdot 10^{-3}$	$2.79 \cdot 10^{-4}$	20/2.8/1.5	32100	1.49
PU-B	$1.75 \cdot 10^{-4}$	$4.02 \cdot 10^{-3}$	$2.79 \cdot 10^{-4}$	40/2.8/1.5	33400	1.44
PU-C	$1.75 \cdot 10^{-4}$	$6.03 \cdot 10^{-3}$	$2.79 \cdot 10^{-4}$	60/2.8/1.5	36600	1.41

2.4. Self-assembly and gelation of amphiphilic diblock copolymers

Dilute solutions were prepared by dissolving PU-*b*-PTPM in distilled THF which was a common solvent for both blocks with mechanical stirring. Subsequently, anhydrous methanol, which was a poor solvent for PU blocks but good solvent for PTPM blocks, was added to the solution dropwise by a syringe at a rate of 1 drop every 10 s under vigorous stirring to induce formation of polymer micelles with PU as the corona and the hydrophobic block as the core. The micelles were prepared at a polymer concentration of 0.50 wt% in the THF/methanol (w/w: 90/10) mixtures. After 5 h, triethylamine (TEA) as the catalyst (0.4 wt%) was dropped into the above solutions to induce the hydrolysis and condensation of the PTPM blocks in the polymeric aggregates, and then the PTPM blocks were transferred into the crosslinked polysilsesquioxane nanocages. The solution was stirred at room temperature for five days, and thus these organic-inorganic hybrid nanomaterials were obtained conveniently by the sol-gel process.

2.5. Instrumentation

Molecular weight characterization was performed on a HP1100 GPC instrument equipped with a Zorbax HV1618 column connected to a refractive-index detector (G1362A) and a UV detector (G1315A). THF was used as eluent at a flow rate of 1.0 ml/min at 35°C. Polystyrene standards were used for the calibration.

¹H NMR spectra were measured by using a MERCURYPLUS400 (U.S.A. VARIAN) spectrometer. All samples were dissolved in chloroform-D isotope for NMR measurements.

FTIR spectra of the dried copolymer precursor films were recorded on a Nicolet Nexus 470 FTIR spectrometer. All the samples were taken before the gelation step for FTIR, ¹H NMR, GPC measurements.

After gelation, all the samples were dissolved in THF and dropped onto mica flake. After solvent evaporation, the film samples obtained were used for AFM observations. Atomic force microscope (AFM) (Digital Instruments NanoScope IV) was operated with 10×10 μm scanner under tapping mode. AFM imaging technique can provide a representative analysis covering individual micron-

sized particles, such as the diameter and height of particles, surface roughness, etc. [37]. Therefore, the particles that protrude from the polyurethane sample surface may be imaged by using AFM.

The films were finally punched into dog-bone shaped specimens using a punch cutter with a dimension of 55×4×1 mm³ (GB-T13022-1991). The tensile tests were carried out using a CMT4000 Series Floor-standing Electromechanical Universal Testing Machine at room temperature with a crosshead speed of 100 mm/min. Property values reported here represent averaged results of at least five specimens. The thermal decomposition studies were performed from room temperature to 600°C using a Perkin-Elmer Pyris TGA-1 under nitrogen environment at a heating rate of 20°C/min.

3. Results and discussion

3.1. Synthesis and characterization of PU-*b*-PTPM copolymer precursors

GPC traces are shown in Figure 2. Molecular weight is shown on a logarithmic scale and the value of the peak intensity is normalized. The molecular weight (M_w) and the polydispersity (PDI) data obtained are summarized in Table 1. As shown in Figure 2, all the peaks are symmetric, and no shoulder peak was observed, indicating the polymerization occurred as expected. The peak was also shifted gradually to higher molecular weight and the PDI became narrower with the increase of the feed ratio of TPM (Table 1), indicating that the RAFT polymerization occurred and the well controlled copolymers were obtained. Polyurethane prepared by condensation polymerization, as

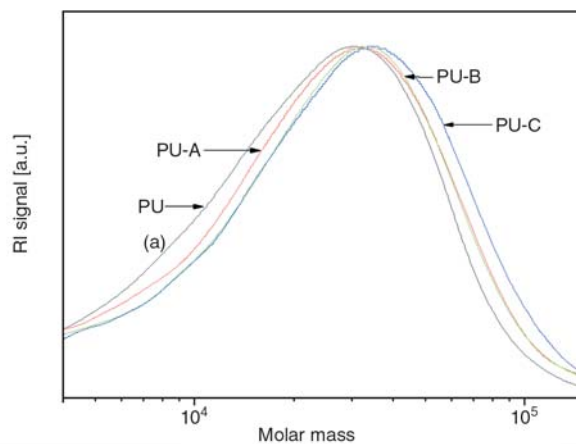


Figure 2. Gel permeation chromatograms of PU and PU-PTPM copolymer precursors

known, has a high PDI. After incorporation of structured TPM block by RAFT polymerization, the PDI decreases with the increase of TPM contents. A gradient growth can also be found as shown in Figure 2 and Table 1, which corresponds to the gradient feed of TPM monomer. According to the M_w results, different TPM chain contents were incorporated into polyurethane, thus obtaining PU-A, PU-B, and PU-C.

Figure 3 shows the ^1H NMR spectra of the copolymer precursors. The chemical shifts appearing at 3.4 ppm are associated with methyl protons of Si-OCH_3 . The H of methylene group adjacent to the oxygen atom of glycol in the PU chain, showed a chemical shift at 3.4–3.5 ppm. The H of the methylene adjacent to the methylene connected with oxygen atom of trimethoxy and the H of the methylene adjacent to the methylene connected with carbonyl in the PU chain showed a chemical shift at 1.60–1.68 ppm. The H of the methylene adjacent to

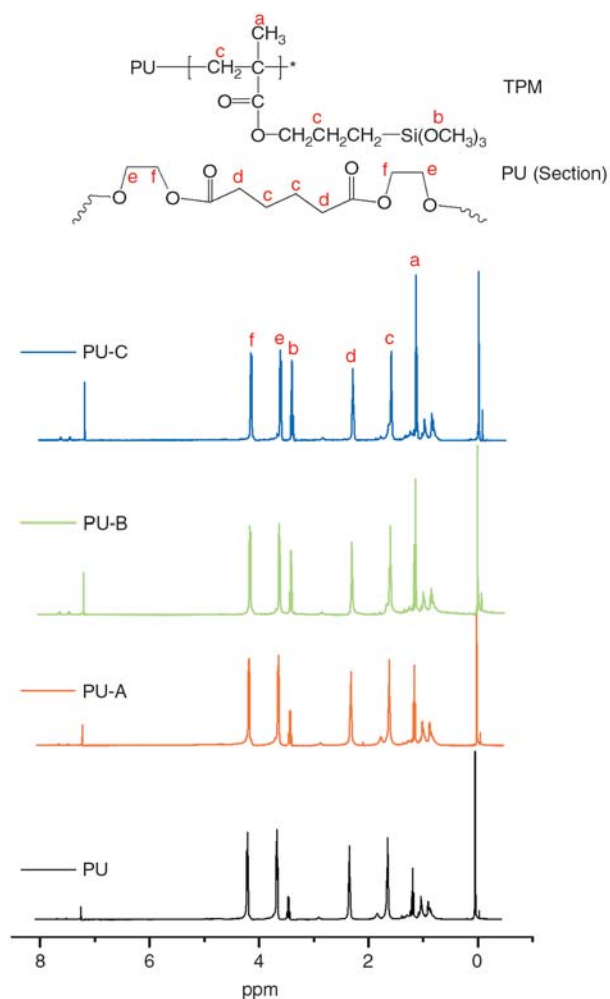


Figure 3. ^1H NMR spectra of PU and PU-PTPM copolymer precursors

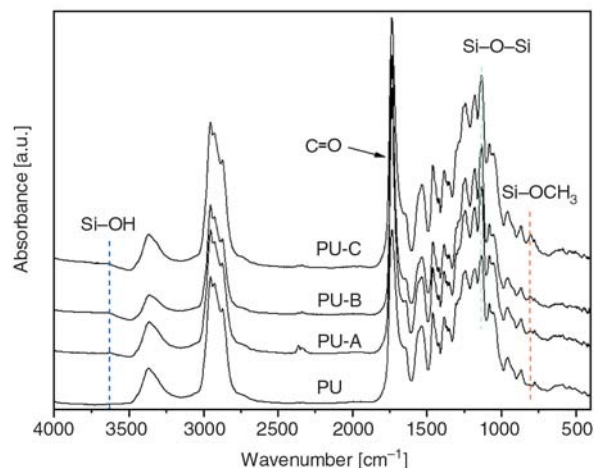


Figure 4. FTIR spectra of PU and PU-PTPM copolymer precursors

the oxygen atom of carbonyl in the PU chain showed a chemical shift at 2.30–2.45 ppm. The H of methyl groups on the cyclohexyl and the H of methyl groups on the TPM exhibited a chemical shift at 1.15–1.25 ppm. Although ^1H NMR spectra of TPM are overlapped with ^1H NMR spectra of polyurethane, gradient increase for chemical shifts at 3.4–3.5 ppm and 1.15–1.25 ppm can still be seen, indicating that a series of block copolymers were successfully prepared with well controlled molecular weights.

The FTIR spectra of PU-PTPM copolymer precursors shown in Figure 4 are generally similar. Gelation of PTPM was easily occurred when exposed to the air, thus we can observe weak Si-OH peaks in FTIR curves. The weak and broad Si-OH band between 3650 and 3500 cm^{-1} is formed in the hydrolysis reaction of the alkoxy groups of TPM. The Si-OH peak at 940 cm^{-1} was overlapped with PU matrix. The peak at 805 cm^{-1} and the peak at 1087 cm^{-1} are probably from the Si-OCH₃ group. The intensity of this peak, appearing in all the hybrid copolymer precursors, increases from PU-A to PU-C, which demonstrates that TPM groups were successfully incorporated into PU via RAFT and the TPM content in the copolymer precursors was gradually increased. Although the characteristic absorption bands of Si-O-Si bond around 1130 cm^{-1} were overlapped with PU matrix, an increased peak intensity was observed due to the condensation of the Si-OH group. The C=O absorption from both the TPM groups and PU can be clearly observed at 1730 cm^{-1} .

3.2. Identification and characterization of PU-silica hybrid materials

The thermal stability of PU was characterized by TGA. The TGA curves of PU and its nanocomposites are shown in Figure 5. The decomposition of PU took place in two stages. The initial step of degradation in stage I is primarily the decomposition of the hard segment, which involves the dissociation of urethane to the original polyol and isocyanate or of the urea group to the original amine and isocyanate, then forms a primary amine, alkyne and carbon dioxide. Stage I occurs at about 200–370°C and is influenced by the content of hard segment. The consequent stage II proceeds by the depolycondensation and polyol degradation mechanisms, and is affected by the content of soft segment. Figure 5 also presents the thermal stability of neat PU and its nanocomposites. When 50% weight loss was selected for comparison, the decomposition temperatures increase from 405°C for neat PU to 423°C for PU-C, indicating the enhancement of thermal stability by incorporating crosslinked silica moiety into PU matrix. The hydrolysis and condensation of alkoxy silane would form crosslinking networks (Si–O–Si) which possess excellent thermal stability over 600°C [25, 33]. The initial decomposition temperature (here taking the temperature at 10% weight loss) of PU-B was about 342°C and higher than that of neat PU (332°C), also suggesting that the thermal stability of the nanocomposite was greatly enhanced compared with neat PU.

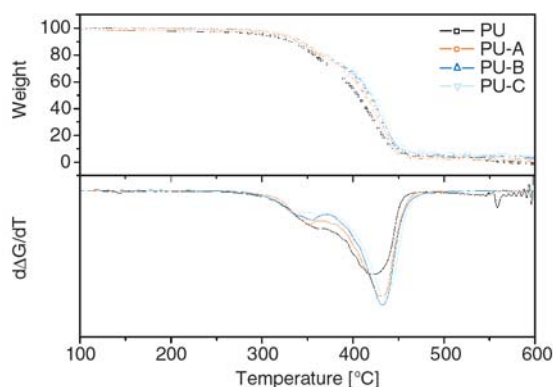


Figure 5. TGA curves of PU and its nanocomposites

Compared to neat PU, the higher residue content of all the nanocomposites at high temperature (600°C) was attributed to the excellent thermal stability of inorganic silica (Si–O–Si) part, which would be accumulated on the surface of the polymer and thus prevent from further thermal decomposition of the inner organic network.

The mechanical properties of PU and its nanocomposites were evaluated by tensile tests at room temperature. The stress-strain curves are shown in Figure 6 and the results obtained are summarized in Table 2. In comparison with the unmodified PU, the TPM-containing nanocomposites exhibited significant increase in both tensile modulus and tensile strength with increasing the TPM content. This increase can be interpreted on the basis of two factors: i) the nano-reinforcement effect from polysilsesquioxane spheres, and ii) the increase in crosslinking density of the networks formed by the hydrolysis and condensation of alkoxy silane [34, 35]. The nano-reinforcement of polysilsesquioxane spheres could be ascribed to the restriction of nano-sized polysilsesquioxane spheres on the deformation of the macromolecular chains. Accordingly, due to the reinforcement, the elongation-at-break also decreases initially with the content of TPM similarly. It may be ascribed to the deformation mechanism of PU [36]. In case of PU composed of hard and soft segment domains, the hard segment domain, sensitive to applied stress, can be tilted

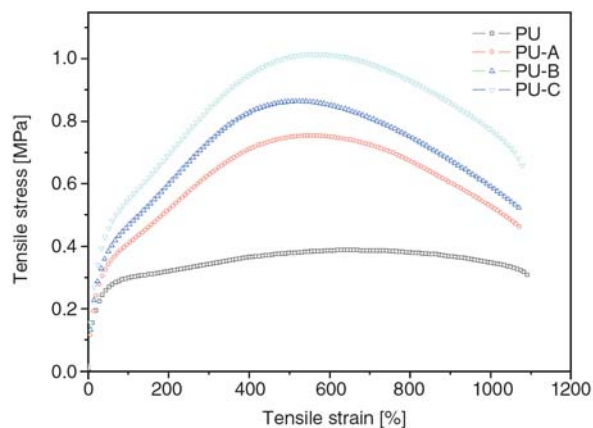


Figure 6. Typical strain–stress curves of PU and its nanocomposites

Table 2. Mechanical properties of synthesized PUs

Sample	Tensile modulus [MPa]	Tensile strength [MPa]	Elongation-at-break [%]
PU	1.43 ± 0.08	0.41 ± 0.02	1372.5 ± 46.7
PU-A	1.61 ± 0.06	0.71 ± 0.04	1032.4 ± 49.7
PU-B	1.75 ± 0.04	0.85 ± 0.02	1004.5 ± 63.9
PU-C	1.95 ± 0.08	0.97 ± 0.04	1038.0 ± 35.9

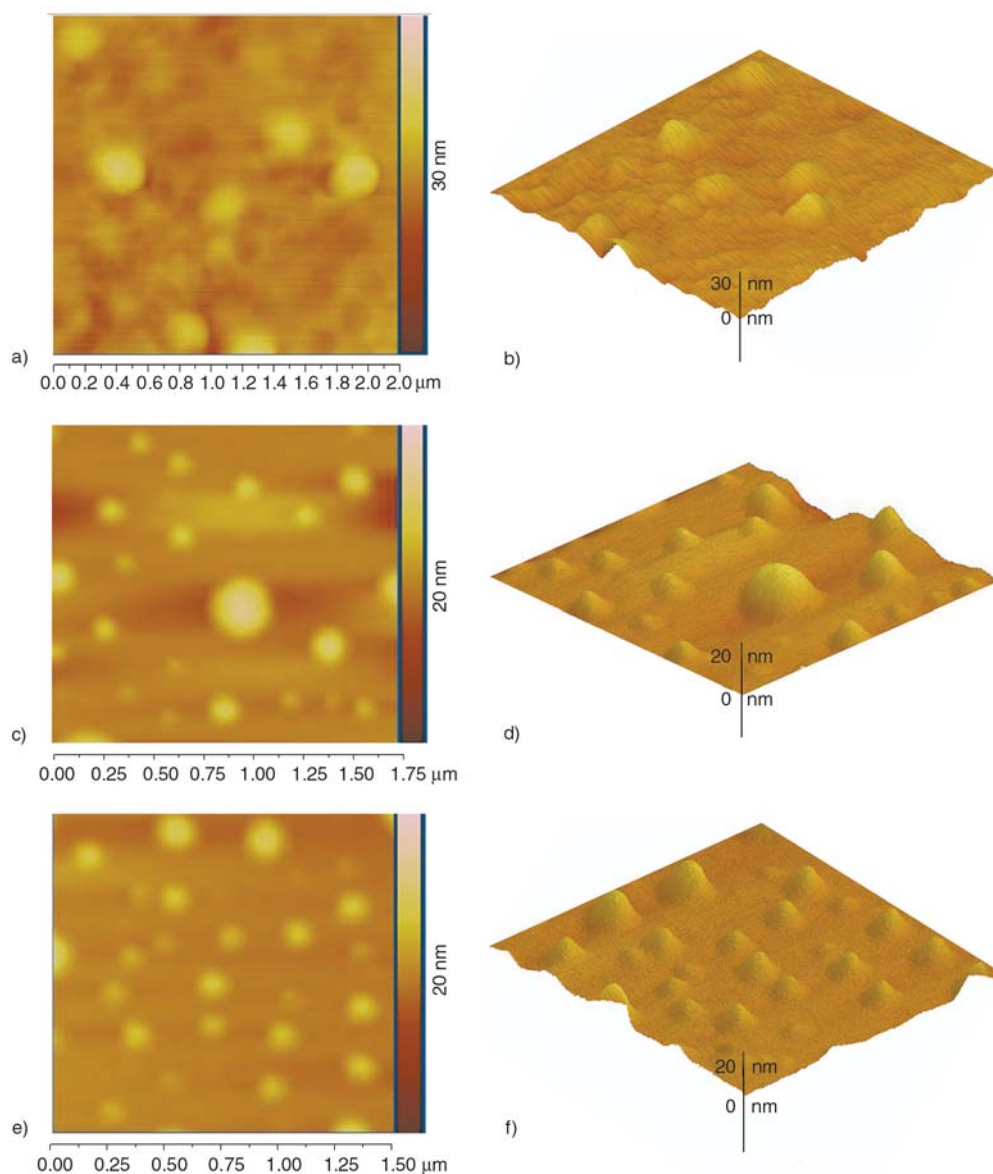


Figure 7. Height-contrast 2D (left) and corresponding 3D (right) AFM images of PU based nanocomposites

toward the stretching direction at low strain; and at high strain, the hard segment domain may align parallel to the stretching direction. Thus, PU can maintain its stress capacity in the relatively high strain without any breakdown of amorphous soft chains. However, the incorporation of polysilsesquioxane spheres hinders the deformation of soft segments in PU and thus leads to lower elongation-at-break.

As shown in Figure 7 from PU-A to PU-C, with increasing the TPM content, the silica spheres undergo a change from lower number with larger diameter to higher number with smaller and homogeneous diameter. The soft surface of polyurethane leads to the unclear image. Moreover, the silica spheres are covered by polyurethane, resulting in

fuzzy boundary of the particles. However, as confirmed by AFM images, the silica spheres with different sizes (about 80–200 nm) are formed during the hydrolysis and condensation. The sphere morphology was influenced by the TPM content in the copolymer. With the increase of TPM incorporation, the silica spheres were smaller and distributed more homogeneously. Thus, the thermal stability and the mechanical properties were enhanced from PU-A to PU-C.

4. Conclusions

In this work, a series of alkoxy-silane-containing copolymers with a gradient change in molecular weight were prepared by RAFT, and PDI became

narrower with the increase of the feed ratio of TPM. After gelation process, the silica particles were uniformly dispersed in the copolymer matrix, and their sizes were in the nanoscale from the AFM results. The thermal stability of the hybrid copolymers was increased with increasing the content of silica spheres. The mechanical property of PU matrix was improved greatly due to the reinforcement effect of polysilsesquioxane nanospheres and the increase in crosslinking density of the silica spheres. Therefore, we can tune the performance of the hybrid nanocomposites by adjusting the configuration of polysilsesquioxane by RAFT polymerization (e.g., via feed ratio).

Acknowledgements

This work is supported by the Shanghai Leading Academic Discipline Project (Project Number: B113).

References

- [1] Dislich H.: New routes to multicomponent oxide glasses. *Angewandte Chemie International Edition*, **10**, 363–369 (1971). DOI: [10.1002/anie.197103631](https://doi.org/10.1002/anie.197103631)
- [2] Zhulina E. B., Borisov O. V.: Self-assembly in solution of block copolymers with annealing polyelectrolyte blocks. *Macromolecules*, **35**, 9191–9203 (2002). DOI: [10.1021/ma020865s](https://doi.org/10.1021/ma020865s)
- [3] Shen H., Eisenberg A.: Control of architecture in block-copolymer vesicles. *Angewandte Chemie International Edition*, **39**, 3310–3312 (2000). DOI: [10.1002/1521-3773\(20000915\)39:18<3310::AID-ANIE3310>3.0.CO;2-2](https://doi.org/10.1002/1521-3773(20000915)39:18<3310::AID-ANIE3310>3.0.CO;2-2)
- [4] Okada A., Usuki A., Kurauchi T., Kamigaito O.: Polymer-clay hybrids. *ACS Symposium Series*, **585**, 55–65 (1995).
- [5] Han Y-H., Taylor A., Mantle M. D., Knowles K. M.: Sol-gel-derived organic-inorganic hybrid materials. *Journal of Non-Crystalline Solids*, **353**, 313–320 (2007). DOI: [10.1016/j.jnoncrysol.2006.05.042](https://doi.org/10.1016/j.jnoncrysol.2006.05.042)
- [6] Jang J., Park H.: *In situ* sol-gel process of polystyrene/silica hybrid materials: Effect of silane-coupling agents. *Journal of Applied Polymer Science*, **85**, 2074–2083 (2002). DOI: [10.1002/app.10747](https://doi.org/10.1002/app.10747)
- [7] Jiang H. M., Zheng Z., Song W. H., Li Z. M., Wang X. L.: Alkoxysilane functionalized polyurethane/poly-siloxane copolymers: Synthesis and the effect of end-capping agent. *Polymer Bulletin*, **59**, 53–63 (2007). DOI: [10.1007/s00289-007-0748-y](https://doi.org/10.1007/s00289-007-0748-y)
- [8] Rodríguez-Hernández J., Chécot F., Gnanou Y., Lecommandoux S.: Toward ‘smart’ nano-objects by self-assembly of block copolymers in solution. *Progress in Polymer Science*, **30**, 691–724 (2005). DOI: [10.1016/j.progpolymsci.2005.04.002](https://doi.org/10.1016/j.progpolymsci.2005.04.002)
- [9] Zhou J. F., Wang L., Dong X. C., Yang Q., Wang J. J., Yu H. J., Chen X.: Preparation of organic/inorganic hybrid nanomaterials using aggregates of poly(stearyl methacrylate)-*b*-poly(3-(trimethoxysilyl) propyl methacrylate) as precursor. *European Polymer Journal*, **43**, 1736–1743 (2007). DOI: [10.1016/j.eurpolymj.2006.09.022](https://doi.org/10.1016/j.eurpolymj.2006.09.022)
- [10] Wu C., Xu T., Yang W.: Synthesis and characterizations of novel, positively charged poly(methyl acrylate)-SiO₂ nanocomposites. *European Polymer Journal*, **41**, 1901–1908 (2005). DOI: [10.1016/j.eurpolymj.2005.02.031](https://doi.org/10.1016/j.eurpolymj.2005.02.031)
- [11] Hsiue G-H., Kuo W-J., Huang Y-P., Jeng R-J.: Microstructural and morphological characteristics of PS-SiO₂ nanocomposites. *Polymer*, **41**, 2813–2825 (2000). DOI: [10.1016/S0032-3861\(99\)00478-4](https://doi.org/10.1016/S0032-3861(99)00478-4)
- [12] Zhang Y. W., Jiang M., Zhao J. X., Wang Z. X., Dou H. J., Chen D. Y.: pH-responsive core-shell particles and hollow spheres attained by macromolecular self-assembly. *Langmuir*, **21**, 1531–1538 (2005). DOI: [10.1021/la047912p](https://doi.org/10.1021/la047912p)
- [13] Pilon L. N., Amies S. P., Findlay P., Rannard S. P.: Synthesis and characterization of shell cross-linked micelles with hydroxy-functional coronas: A pragmatic alternative to dendrimers? *Langmuir*, **21**, 3808–3813 (2005). DOI: [10.1021/la047046g](https://doi.org/10.1021/la047046g)
- [14] Zhao Q., Han B., Wang Z., Gao C., Peng C., Shen J.: Hollow chitosan-alginate multilayer microcapsules as drug delivery vehicle: Doxorubicin loading and in vitro and in vivo studies. *Nanomedicine: Nanotechnology, Biology and Medicine*, **3**, 63–74 (2007). DOI: [10.1016/j.nano.2006.11.007](https://doi.org/10.1016/j.nano.2006.11.007)
- [15] Du J., Chen Y.: Atom-transfer radical polymerization of a reactive monomer: 3-(trimethoxysilyl)propyl methacrylate. *Macromolecules*, **37**, 6322–6328 (2004). DOI: [10.1021/ma0359382](https://doi.org/10.1021/ma0359382)
- [16] Du J. Z., Chen Y. M.: Organic-inorganic hybrid nanoparticles with a complex hollow structure. *Angewandte Chemie*, **116**, 5194–5197 (2004). DOI: [10.1002/ange.200454244](https://doi.org/10.1002/ange.200454244)
- [17] Du J., Chen Y., Zhang Y., Han C. C., Fischer K., Schmidt M.: Organic/inorganic hybrid vesicles based on a reactive block copolymer. *Journal of the American Chemical Society*, **125**, 14710–14711 (2003). DOI: [10.1021/ja0368610](https://doi.org/10.1021/ja0368610)
- [18] Sayari A., Hamoudi S.: Periodic mesoporous silica-based organic-inorganic nanocomposite materials. *Chemistry of Materials*, **13**, 3151–3168 (2001). DOI: [10.1021/cm011039l](https://doi.org/10.1021/cm011039l)

- [19] Du J. Z., Chen Y. M.: Preparation of organic/inorganic hybrid hollow particles based on gelation of polymer vesicles. *Macromolecules*, **37**, 5710–5716 (2004). DOI: [10.1021/ma0497097](https://doi.org/10.1021/ma0497097)
- [20] Park J-W., Thomas E. L.: A Surface-reactive rod-coil diblock copolymer: Nano- and micropatterned polymer brushes. *Journal of the American Chemical Society*, **124**, 514–515 (2002). DOI: [10.1021/ja017116v](https://doi.org/10.1021/ja017116v)
- [21] Park J-W., Thomas E. L.: Multiple ordering transitions: Hierarchical self-assembly of rod-coil block copolymers. *Advanced Materials*, **15**, 585–588 (2003). DOI: [10.1002/adma.200304591](https://doi.org/10.1002/adma.200304591)
- [22] Du J. Z., Chen Y. M.: Organic-inorganic hybrid nanoparticles with a complex hollow structure. *Angewandte Chemie International Edition*, **43**, 5084–5087 (2004). DOI: [10.1002/anie.200454244](https://doi.org/10.1002/anie.200454244)
- [23] Ni H., Aaserud D. J., Simonsick W. J. Jr., Soucek M. D.: Preparation and characterization of alkoxysilane functionalized isocyanurates. *Polymer*, **41**, 57–71 (2000). DOI: [10.1016/S0032-3861\(99\)00160-3](https://doi.org/10.1016/S0032-3861(99)00160-3)
- [24] Kannan R. Y., Salacinski H. J., De Groot J., Clatworthy J. I., Bozec L., Horton M., Butler P. E., Seifalian A. M.: The antithrombogenic potential of a polyhedral oligomeric silsesquioxane (POSS) nanocomposite. *Biomacromolecules*, **7**, 215–223 (2006). DOI: [10.1021/bm050590z](https://doi.org/10.1021/bm050590z)
- [25] Liu Y., Ni Y., Zheng S.: Polyurethane networks modified with octa(propylglycidyl ether) polyhedral oligomeric silsesquioxane. *Macromolecular Chemistry and Physics*, **207**, 1842–1851 (2006). DOI: [10.1002/macp.200600241](https://doi.org/10.1002/macp.200600241)
- [26] Hua D. B., Sun W., Bai R. K., Lu W. Q., Pan C. Y.: Study on controlled/living free-radical polymerization of methyl acrylate in the presence of benzyl 9H-carbazole-9-carbodithioate under thermal condition. *European Polymer Journal*, **41**, 1674–1680 (2005). DOI: [10.1016/j.eurpolymj.2005.01.022](https://doi.org/10.1016/j.eurpolymj.2005.01.022)
- [27] Charleux B., Nicolas J., Guerret O.: Theoretical expression of the average activation-deactivation equilibrium constant in controlled/living free-radical copolymerization operating via reversible termination. Application to a strongly improved control in nitroxide-mediated polymerization of methyl methacrylate. *Macromolecules*, **38**, 5485–5492 (2005). DOI: [10.1021/ma050087e](https://doi.org/10.1021/ma050087e)
- [28] Xia J., Zhang X., Matyjaszewski K.: Synthesis of star-shaped polystyrene by atom transfer radical polymerization using an ‘arm first’ approach. *Macromolecules*, **32**, 4482–4484 (1999). DOI: [10.1021/ma9900378](https://doi.org/10.1021/ma9900378)
- [29] Chiefari J., Mayadunne R. T. A., Moad C. L., Moad G., Rizzardo E., Postma A., Skidmore M. A., Thang S. H.: Thiocarbonylthio compounds (SC(Z)S-R) in free radical polymerization with reversible addition-fragmentation chain transfer (RAFT polymerization). Effect of the activating group Z. *Macromolecules*, **36**, 2273–2283 (2003). DOI: [10.1021/ma020883+](https://doi.org/10.1021/ma020883+)
- [30] Pyun J., Matyjaszewski K.: Synthesis of nanocomposite organic/inorganic hybrid materials using controlled/‘living’ radical polymerization. *Chemistry of Materials*, **13**, 3436–3448 (2001). DOI: [10.1021/cm011065j](https://doi.org/10.1021/cm011065j)
- [31] Smulders W., Gilbert R. G., Monteiro M. J.: A kinetic investigation of seeded emulsion polymerization of styrene using reversible addition-fragmentation chain transfer (RAFT) agents with a low transfer constant. *Macromolecules*, **36**, 4309–4318 (2003). DOI: [10.1021/ma026020y](https://doi.org/10.1021/ma026020y)
- [32] Le T. P., Moad G., Rizzardo E., Thang S. H.: Polymerization with living characteristics. PCT International Application, WO9801478 AI 980115 (1998).
- [33] Liu P., Song J., He L., Liang X., Ding H., Li Q.: Alkoxysilane functionalized polycaprolactone/poly-siloxane modified epoxy resin through sol-gel process. *European Polymer Journal*, **44**, 940–951 (2008). DOI: [10.1016/j.eurpolymj.2007.12.014](https://doi.org/10.1016/j.eurpolymj.2007.12.014)
- [34] Cho J. W., Lee S. H.: Influence of silica on shape memory effect and mechanical properties of polyurethane-silica hybrids. *European Polymer Journal*, **40**, 1343–1348 (2004). DOI: [10.1016/j.eurpolymj.2004.01.041](https://doi.org/10.1016/j.eurpolymj.2004.01.041)
- [35] Nomura Y., Sato A., Sato S., Mori H., Endo T.: Synthesis of novel moisture-curable polyurethanes end-capped with trialkoxysilane and their application to one-component adhesives. *Journal of Polymer Science Part A: Polymer Chemistry*, **45**, 2689–2704 (2007). DOI: [10.1002/pola.22025](https://doi.org/10.1002/pola.22025)
- [36] Valentová H., Sedláková Z., Nedbal J., Ilavský M.: Formation, structure, thermal and dynamic mechanical behaviour of ordered polyurethane networks based on mesogenic diol. *European Polymer Journal*, **37**, 1511–1517 (2001). DOI: [10.1016/S0014-3057\(01\)00017-9](https://doi.org/10.1016/S0014-3057(01)00017-9)
- [37] Uricanu V., Donescu D., Banu A. G., Serban S., Olteanu M., Dudau M.: Organic-inorganic hybrids made from polymerizable precursors. *Materials Chemistry and Physics*, **85**, 120–130 (2004). DOI: [10.1016/j.matchemphys.2003.12.024](https://doi.org/10.1016/j.matchemphys.2003.12.024)